buildings

MDPI

Article

The Dimensional Stability and Bonding Performance of Hybrid CLT Fabricated with Lumber and COSB

Zhijun Liang [1], Guojun Chen [1], Yi Wang [1], Zhiqiang Wang [1,*] and Meng Gong [2]

[1] College of Materials Science and Engineering, Jiangsu Co-Innovation Center of Efficient Processing and Utilization of Forest Resources, Nanjing Forestry University, 159 Longpan Road, Nanjing 210037, China
[2] Wood Science and Technology Centre, University of New Brunswick, 1350 Regent Street, Fredericton, NB E3C 2G6, Canada
* Correspondence: wangzhiqiang@njfu.edu.cn

Abstract: The differences of physical and mechanical properties of different laminations, such as softwood, hardwood or other structural composite lumber, in hybrid cross-laminated timber (HCLT), lead to their dimensional stability and bonding performance more complex than generic cross-laminated timber (CLT). In this paper, the spruce-pine-fir (SPF) dimension lumber and construction oriented strand board (COSB) were employed to fabricate HCLT. The effects of four configurations and three adhesives on the dimensional stability and bonding performance of CLT and HCLT were evaluated in term of the water absorption (WA), thickness swelling (TS), block shear strength (BSS), wood failure percentage (WFP) and rate of delamination (RD). The results showed that with the increase of the COSB laminations, the WA of HCLT specimens decreased, and the values of TS, BBS and WFP increased. The configuration had a significant influence on the dimensional stability, BBS and WFP of the specimen. The adhesive had a significant influence on the dimensional stability and some bonding performances of the specimen. The phenol resorcinol formaldehyde (PRF) specimens had the lowest average RD value compared with the one-component polyurethane (PUR) and emulsion polymer isocyanate (EPI) specimens. Failures were prone to occur in the middle of the thickness of COSB lamination during block shear and delamination tests. The outcome of this paper could help the engineering application of HLCT.

Keywords: hybrid cross-laminated timber; construction oriented strand board; dimensional stability; bonding performance; delamination

check for updates

Citation: Liang, Z.; Chen, G.; Wang, Y.; Wang, Z.; Gong, M. The Dimensional Stability and Bonding Performance of Hybrid CLT Fabricated with Lumber and COSB. *Buildings* **2022**, *12*, 1669. https://doi.org/10.3390/buildings12101669

Academic Editor: Karim Ghazi Wakili

Received: 4 September 2022
Accepted: 2 October 2022
Published: 12 October 2022

1. Introduction

In recent years, more and more mid-rise and high-rise timber buildings employed cross-laminated timber (CLT) as the wall, floor and roof elements. The annual global production of CLT increased exponentially, from 50,000 m^3 in 2000 to 625,000 m^3 in 2014, and is expected to reach 3,000,000 m^3 by 2025 [1]. At present, CLT is mostly manufactured using softwoods, such as European spruce and North America SPF (spruce-pine-fir) dimension lumber. Recently, some studies are carrying out to fabricate hybrid CLT (HCLT) with hardwoods, structural composite lumber (SCL) or structural panels, in order to improve the mechanical properties of CLT and expand the sources of CLT laminations. The SCL and structural panels that have been studied include laminated veneer lumber (LVL), laminated strand lumber (LSL), oriented strand lumber (OSL), oriented strand board (OSB) and plywood [2–4]. These researches show that adding SCL or structural panels to CLT can improve the production efficiency, fire resistance and mechanical properties of CLT, due to their high mechanical properties, low variability of physical and mechanical properties, and large product size [5].

The bonding quality will affect the stress transfer between CLT laminations [6]. Poor bonding quality will lead to the decline of mechanical properties of CLT and the failure of bonding line, rather than bending or shear failures [7,8]. At present, the researches on CLT bonding performance mainly focus on: (1) the influences of bonding process parameters, such as the adhesive, spreading rate, pressing time, temperature and pressure. For example, the studies of Sikora et al. [9] and Liao et al. [10] showed that the penetration of the adhesive became deeper and the bonding durability of the adhesive became better as the CLT bonding pressure became greater. Yusof et al. [11] studied the manufacture process of *Acacia mangium* CLT and found that when the density of sawn timber was large, high pressure can improve the permeability of the adhesive, thereby improving the bonding strength. Wetzig [12] found that the thick one component polyurethane adhesive (PUR) bonding line has high ductility, which helped to absorb the expansion and contraction stress of hardwood, so as to improve rate of delamination (RD). Santos et al. [13] showed that increasing bonding pressure significantly enhances the WFP after delamination tests, while the delamination and the shear strength seems not to be significantly affected. Knorz et al. [14] also found that the bonding pressure had no influence on results of the delamination test. (2) the influences of physical characteristics of wood, such as density, moisture content, microstructure, porosity, surface quality, etc. [6,9–12,15]. Song et al. [15] utilized larch to produce 3-layer CLT, and investigated the influence of the annual ring angle of sawn timber on the bonding interface performance. The results showed that when the directions of annual rings of the outer lamination were outward, the RD was the highest, which should be avoided in CLT production. Wood density is the main factor affecting bonding strength and wood failure percentage (WFP). Therefore, the addition of hardwood or SCL into HCLT will create new bonding problems due to the various density, bonding interfaces, internal structure, and dimensional stability of various lamination materials. These bonding issues will become more prominent in the humid conditions [6].

Wood will shrink and swell with the change of environmental humidity. The effect of shrinkage and swelling of wood components in high-rise timber buildings will be significant due to accumulation, and then affects the stability of the building structure. As the structural component in mid-rise and high-rise timber building, the dimension of CLT will change under different humidity conditions. Due to the orthogonal structure, the dimensional expansions coefficient of CLT in thickness, width and length directions are significantly different from those of solid wood or glulam. For example, in the width direction, the dimensional expansion coefficient of CLT is less than 1/5 of that of solid wood or glulam; in the length direction, however, it is three times that of solid wood or glulam; and it is slightly higher than that of solid wood or glulam in the thickness [16]. Both the wood species, thickness of lamination, and adhesive of CLT can affect its thickness expansion. Yusof et al. [17] discovered that the average thickness swelling (TS) of *Acacia mangium* CLT made from PRF and PUR adhesives were 1.053% and 0.696%, respectively, and the effect of adhesive was significant. The water absorption (WA) of the coconut wood CLT was between 20–11% and has a highly negative linear relationship with density. However, no linear relationship was found between TS and density, with an average TS of 2.4% [18]. In addition, the SCL or structural panels are compressed and formed through hot pressing, which is prone to thickness expansion in the humid environment. This brings challenges to the dimensional stability of HCLT made by SCL or structural panels, especially for the WA and TS.

At present, the researches of HCLT, especially the HCLT made by SCL and sawn timber, mainly focus on their mechanical properties. There are limited researches on their dimensional stability and bonding performance. In our previous study, the short-term and long-term mechanical properties of HCLT, fabricated with SPF dimension lumber and construction OSB (COSB) with different configurations, have been evaluated by experiments and finite element modelling. It was found the addition of COSB improved the short-term and long-term flexural and shear mechanical properties of CLT [19,20]. This study further evaluated the effect of the configuration and adhesive on the dimensional stability and bonding performance of HCLT. The results of this study will provide basic data for the engineering application of the HCLT.

2. Materials and Methods

2.1. Materials

In this study, No.2 SPF dimension lumber from Canada and COSB panel from China were employed as lamination materials. COSB is made of three layers of strands where the strands are oriented orthogonally between adjacent layer. For example, the strands in the surface and bottom layers are oriented parallelly to the length direction of COSB, which called major direction. However, the strands in the core layer are oriented parallelly to the width direction of COSB, which called minor direction. The dimension of COSB is 2440 mm × 1220 mm × 24 mm (length × width × thickness), and the average moisture content and density of COSB are 4.8% and 720 kg/m^3, respectively. The dimension of SPF is 3600 mm × 89 mm × 38 mm (length × width × thickness), and the average moisture content and density of SPF are 14% and 410 kg/m^3, respectively.

Three structural adhesives, namely one-component polyurethane (PUR), emulsion polymer isocyanate (EPI), and phenol resorcinol formaldehyde (PRF), were chosen to bond CLT and HCLT in this study. The PUR adhesive (Icema® R645/30) provided by H.B. Fuller (Shanghai, China) has a viscosity of 24,000 mPa·s and a solid content of 100%. A mixture of polyvinyl alcohol (PVA) water-based emulsion, filler and additives with a viscosity of 6250 ± 1250 mPa·s and solid content of 58 ± 1% (Prefere 6151), as well as an isocyanate hardener (Prefere 6651), were acquired from Dynea (Shanghai, China) to make up the EPI adhesive. The PRF adhesive consists of paraformaldehyde (PFA) compound power (PRH-10A) and phenol-resorcinol emulsions (PR-1HSE), having a viscosity of 15,000 mPa·s. and solid content of 65%, purchased from AICA (Shanghai, China).

2.2. CLT and HCLT Configurations

The 3-layer CLT and HCLT specimen were fabricated with various layers of COSB and SPF dimension lumber, resulting into four configurations of specimen (configuration A, B, C, and D), Table 1. In addition, three adhesives (PUR, EPI and PRF) were applied to glue the specimens, respectively, resulting a total of twelve groups of specimens were obtained. The specimen number is expressed as "adhesive—configuration". For example, "PUR-A" indicates that the used adhesive is PUR and the configuration of the specimen is A.

Table 1. CLT and HCLT configurations.

Configuration Type	Lamination Material	Thickness Ratio of COSB	Lamination Orientation
A	T-T-T	0	
B	T-O-T [1]	33%	$\|$-$\perp$-$\|$ [2]
C	O-T-O	66%	
D	O-O-O	100%	

[1] T = SPF, O = COSB. [2] $\|$ = longitudinal orientation, $\perp$ = transverse orientation.

2.3. CLT and HCLT Specimen Preparation

The thickness of SPF dimension lumber was firstly processed to the same thickness of COSB (24 mm) and then the surface of SPF and COSB were cleaned. 90 g/m^2 of water were sprayed to the surface of COSB to ensure the bonding quality [19]. All CLT and HCLT panels are pressed at room temperature about 20 °C according to the instructions of the adhesive manufacturer. The applied pressing pressure for all specimen is 1.0 MPa. The spreading rate and pressing time of PUR was 200 ± 10 g/m^2 and 180 min, respectively. For EPI and PRF, the mass ratio of main agent and curing agent was 100:20 based on the manufacturers' recommendation. The spreading rate and pressing time of EPI and PRF are 270 ± 10 g/m^2 and 140 min, 250 ± 10 g/m^2 and 420 min, respectively. The final dimensions of 3-layer CLT and HCLT panels is 420 × 420 × 72 mm^3 (length × width × thickness), and a total of twenty CLT and HCLT panels are prepared. All the CLT and HCLT panels were conditioned under a relative humidity (RH) of 65% and 20 °C for more than 14 days and then were processed to various test specimens for further tests, Table 2.

Table 2. Dimension and number of specimens.

Test Type	Dimension (Length × Width × Thickness) mm	Number of Specimens
Water absorption and thickness swelling	100 × 100 × 72	60
Block shear	40 × 40 × 72	240
Delamination	100 × 100 × 72	240

2.4. Test Methods

2.4.1. Water Absorption and Thickness Swelling Tests

The WA and TS of CLT and HCLT specimens were evaluated according to ASTM D1037 [21]. Measuring the change in mass and average thickness of the specimen before and after immersion in a constant temperature water bath at pH = 7 ± 1 and 20 ± 1 °C for 24 h. Then the WA and TS of the specimens can be calculated by related equations.

2.4.2. Block Shear Test

The dry and wet block shear strength (BSS) were tested according to EN16351-2015 [22] and GB/T 50329-2012 [23], respectively. Before the dry BSS test, the specimen was placed in a constant temperature and humidity box at 20 °C and a relative humidity of 65% until its mass was stable. For the wet BSS test, however, the specimen was firstly immersed in water at a temperature of 20 °C for 24 h and then was tested by block shearing.

The BSS test was carried out under displacement control at a rate of 5 mm/min. After test of the first bonding line, the specimen was rotated 90° and then the second bonding line was tested [22]. The test setup is shown in Figure 1. The BSS of each specimen was defined as the mean BSS value of its two bonding lines. The BSS of individual bonding line was calculated by Equation (1). The WFP of the bonding line was also estimated, and the WFP value of each specimen was defined as the mean WFP value of its two bonding lines.

$$f = \frac{F\text{max}}{A} \tag{1}$$

where f is the block shear strength, MPa; F_{max} is the ultimate load, N; A is the shear area of bonding line, mm^2.

Figure 1. Test setup of block shear tests.

2.4.3. Delamination Test

Delamination tests were carried out in accordance with GB/T 26899-2011 to determine the RD of the specimen [24]. The initial mass and length of bonding lines in the perimeters of each delamination specimen were measured firstly. The specimens were then treated with two different conditions, i.e., impregnation and boiling conditions, respectively. During the process of impregnation condition, the specimens were completely immersed in room temperature water (about 25 °C) for 24 h and were then placed in a drying oven to be further air-dried at 65–75 °C until achieving between 100–110% of their initial mass. The specimens treated with boiling condition, however, were firstly immersed in boiling water and room temperature water (about 25 °C) successively for 4 h and 1 h, respectively. And the specimens were then placed in a drying oven to be further air-dried at 65–75 °C until achieving between 100–110% of their initial mass. Each treatment of impregnation or boiling condition included two cycles, and after each cycle, the total RD of each specimen was calculated by Equation (2).

$$\mathrm{RD} = \frac{l}{L} \times 100\% \tag{2}$$

where l is the total delamination length of each specimen (mm), and L is the total perimeters of all bonding lines of each delamination specimen (mm).

3. Results and Discussion

The dimensional stability and bonding performance of all specimens are summarized in Table 3.

Table 3. Experimental results for all specimens.

Specimen	WA (%)	TS (%)	BSS (MPa)		WFP (%)		RD (%)			
							Impregnation		Boiling	
			Dry	Wet	Dry	Wet	1 Cycle	2 Cycles	1 Cycle	2 Cycles
PUR-A	13.07 (4.56)	2.20 (13.52)	1.79 (10.90)	1.54 (6.02)	83 (13.80)	58 (45.26)	5.36 (91.85)	10.71 (31.20)	6.91 (81.23)	13.52 (53.12)
PUR-B	10.23 (10.15)	2.47 (14.91)	3.59 (8.08)	2.79 (15.42)	97 (8.55)	95 (9.92)	2.40 (84.58)	8.75 (65.08)	5.63 (96.11)	11.16 (55.06)
PUR-C	10.06 (6.44)	2.62 (18.21)	3.15 (9.70)	2.05 (15.95)	95 (6.51)	72 (23.83)	2.49 (103.14)	6.14 (74.71)	5.90 (57.53)	12.76 (82.17)
PUR-D	8.02 (13.25)	3.20 (11.73)	4.20 (12.78)	2.94 (8.87)	100 (0.00)	100 (0.00)	2.37 (63.03)	7.62 (51.41)	6.94 (72.42)	8.11 (75.62)
EPI-A	16.72 (12.64)	2.06 (19.54)	2.01 (13.00)	1.74 (8.29)	77 (21.07)	56 (40.78)	5.12 (63.03)	7.71 (59.92)	7.40 (106.20)	13.71 (76.03)
EPI-B	13.50 (5.48)	2.14 (8.12)	3.38 (7.91)	2.77 (6.90)	91 (11.83)	84 (16.42)	4.74 (75.00)	10.10 (43.51)	6.33 (77.73)	15.75 (36.08)
EPI-C	11.06 (7.86)	2.43 (6.09)	3.52 (9.93)	2.70 (10.64)	91 (5.68)	86 (16.81)	3.77 (129.01)	11.84 (40.88)	10.16 (60.98)	17.20 (74.86)
EPI-D	9.35 (14.44)	3.50 (14.20)	4.12 (18.09)	2.91 (12.44)	98 (3.56)	96 (6.65)	3.68 (104.21)	12.51 (57.66)	7.46 (31.45)	16.04 (62.08)
PRF-A	12.99 (11.29)	1.80 (21.16)	1.86 (7.32)	1.62 (6.61)	66 (14.93)	69 (17.10)	3.22 (97.95)	6.03 (66.17)	7.97 (65.14)	9.75 (59.47)
PRF-B	10.18 (13.90)	2.03 (7.84)	3.12 (8.04)	2.33 (6.74)	82 (10.11)	73 (14.82)	1.56 (109.75)	4.24 (79.71)	3.70 (147.69)	6.76 (93.34)
PRF-C	9.39 (10.50)	2.06 (19.10)	3.28 (14.23)	2.66 (6.09)	87 (10.26)	75 (14.71)	2.05 (142.11)	2.82 (136.71)	3.77 (111.99)	7.84 (74.59)
PRF-D	7.84 (12.01)	2.15 (15.92)	4.41 (10.44)	3.65 (4.64)	100 (0.00)	100 (0.00)	1.33 (138.32)	2.25 (259.90)	2.73 (147.68)	5.46 (133.50)

Value in ( ) is the coefficient of variation (%).

3.1. Dimensional Stability

3.1.1. Water Absorption

The effect of different configurations on the WA of specimen is presented in Figure 2a. The WA of the specimen, bonded with various adhesives, decreased with the increase of the thickness ratio of COSB in HCLT. For example, compared with the specimen PUR-A, the average WA of the HCLT specimen (specimen PUR-B, PUR-C, PUR-D) decreased 21.73%, 23.03% and 38.64%, respectively. Da Rosa et al. [25] found that the WA was inversely proportional to the panel density, and the smaller the panel density, the greater the WA. In this study, the density of SPF dimension lumber is only 56.94% of COSB. There are many pores in SPF dimension lumber, and moisture can easily enter from the pores of the wood. In addition, the adhesive and other additives in COSB, such as paraffin, can keep water out, which resulting low WA of COSB. In conclusion, an increase in the thickness ratio of COSB layers will lead to a decrease in the WA of HCLT. For different configurations, one-component PUR has the most significant effect on water absorption, which may be due to the poor water resistance of PUR.

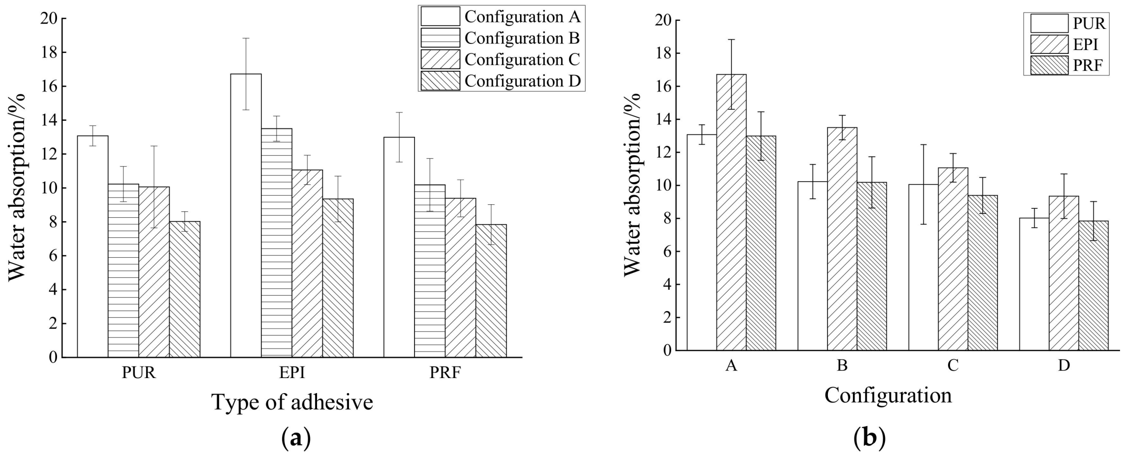

Figure 2. WA of CLT and HCLT specimens: (**a**) Influence of configuration, and (**b**) Influence of adhesive.

The adhesive also affected the WA of specimen, Figure 2b. The EPI specimen showed the highest value of WA. For the configuration A, B and C, large difference of WA of various specimen were found and the EPI specimen had the highest WA. The WA of EPI specimen with configuration A is 27.93% and 28.71% higher than those of the PUR and PRF specimens, respectively. For the configuration D, however, the difference in WA of the three adhesive specimens was small. Results showed that the average WA of all specimens for the three adhesives (PUR, EPI and PRF) were 10.35%, 12.66% and 10.10%, respectively. And for different adhesives, configuration B has the most significant effect on water absorption.

3.1.2. Thickness Swelling

The influence of configuration on the TS of specimen is shown in Figure 3a. With the increase of thickness ratio of COSB layers in HCLT, the TS of specimen increased, which is contrary to the effect of configuration on the WA. For instance, the specimen PUR-D had the lowest WA and the highest TS in all PUR specimens. The strands of COSB panel are compressed by hot pressing. After absorbing water, the strands will rebound to a certain extent, resulting in a larger TS of COSB panel. The dimensional stability (TS and WA) of OSB is mainly determined by its density, strand configuration and degree of bonding [26]. The COSB has higher density and compression than OSB to obtain high mechanical properties, so the TS is more likely to occur in COSB.

The effect of adhesive on the TS is shown in Figure 3b. Among all the configurations, the PRF specimen had the lowest TS. For example, for configuration A, the average TS of PRF specimen was 18.18% and 12.62% lower than those of the PUR and EPI specimens, respectively. In addition, for the three configurations (A, B and C), the TS of the PUR specimen is the largest, followed by the EPI specimen, and the smallest is the PRF specimen. Yusof et al. [11] studied the TS of *Acacia mangium* CLT bonded with PUR or PRF adhesives, and found that the TS of PRF specimens was 33.9% lower than that of PUR specimens. This is because PRF, unlike PUR, can penetrate into the wood cell wall to ensure stronger covalent bonds, and better resistance to water swelling is obtained. Therefore, when the PRF adhesive is exposed to water, there is less expansion, resulting in less stress and displacement of the adhesive [27]. For example, the TS of specimen PRF-D was only 2.15%, which is very close to that of specimen PUR-A (2.2%). This indicates that the excellent water swelling resistance of PRF adhesive counteracted the TS of COSB lamination.

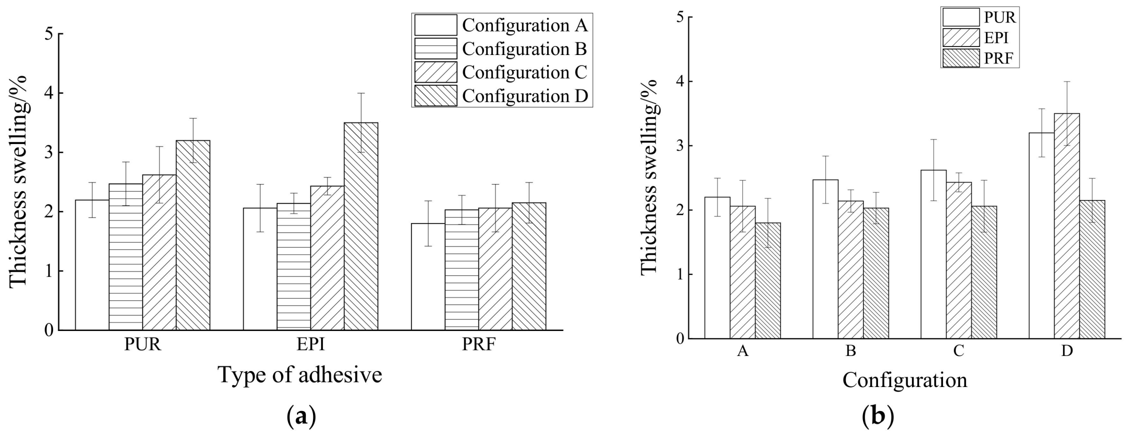

Figure 3. TS of CLT and HCLT specimens: (**a**) Influence of configuration, and (**b**) Influence of adhesive.

The ANOVA results of dimensional stability shown that both factors, i.e., configuration and adhesive, had a significant influence on the WA and TS of specimen, and the interaction between these two factors also had a significant influence, Table 4.

Table 4. ANOVA results of dimensional stability.

	Source of Variance	df	Mean Square	Significant Level
Water absorption	configuration	3	64.807	***
	adhesive	2	22.925	***
	configuration × adhesive	6	5.339	*
Thickness swelling	configuration	3	2.401	***
	adhesive	2	2.168	***
	configuration × adhesive	6	0.407	*

* = significant at 5% level, ** = significant at 1% level, *** = significant at 0.1% level.

3.2. Bonding Performance

3.2.1. Block Shear Strength

The BSS and WFP of specimens at dry condition are shown in Figure 4. For the specimen bonded with the same adhesive, the addition of COSB significantly improved the BSS, Figure 4a. The average BSS of the COSB CLT specimen (configuration D) was 4.24 MPa, which was 2.25 times that of the SPF CLT specimen(configuration A). The specimens of configurations B and C have similar BSS, with average values of 3.36 MPa and 3.32 MPa, respectively. This is because they have the same bonding interface, both of which are COSB-SPF bonding lines. In addition, the characteristic values of BSS at dry condition of normal CLT and HCLT were 1.47MPa and 2.53MPa, respectively, which meet the requirements of EN 16351-2015 [20]. The effect of adhesive on BSS is shown in Figure 4b. For the same configuration, the BSS of the three adhesives (PUR, EPI and PRF) are similar, and their average values are 3.18 MPa, 3.26 MPa, and 3.17 MPa, respectively.

The WFP of specimen at dry condition has the similar tendency as the BSS, Figure 4. The WFP of COSB CLT specimen (configuration D) was the highest, closing to 100%. There was a slight decrease in WFP of the HCLT specimen (configurations B and C), which were above 80%. So the WFP of specimen of configurations B, C and D meet the WFP requirements in EN 16351-2015 [22]. However, the SPF CLT specimen (configuration A) had the lowest WFP in the four configurations.

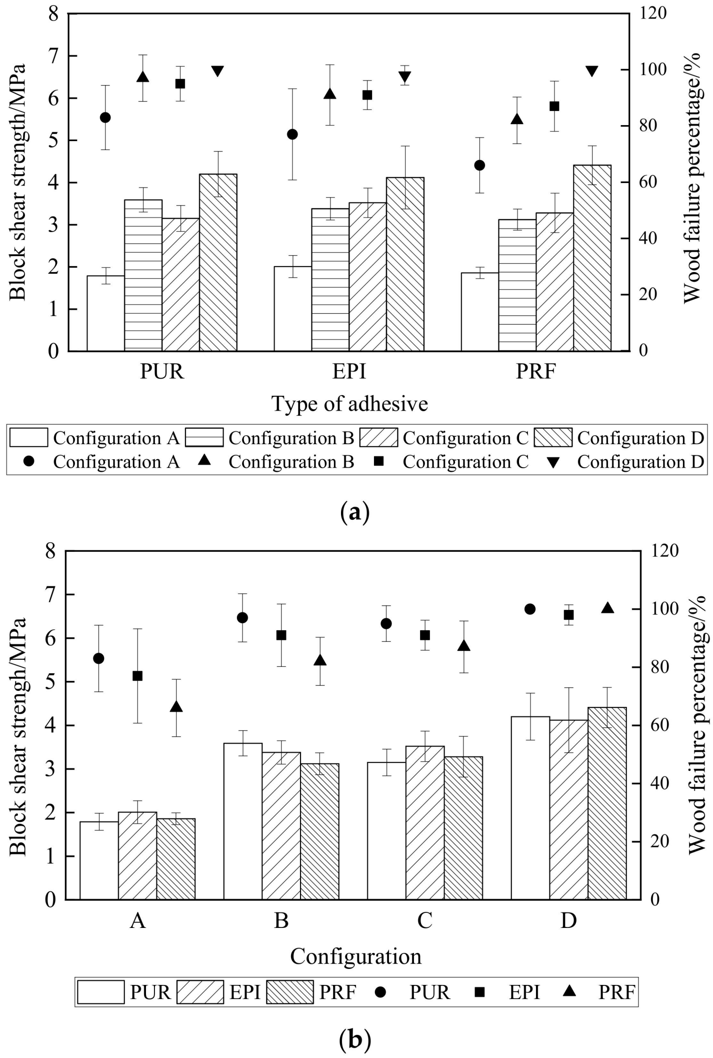

Figure 4. BSS and WFP of CLT and HCLT specimens at dry condition: (**a**) Influence of configuration, and (**b**) Influence of adhesive.

The BSS and WFP of specimens at wet condition are presented in Figure 5. The influence of the configuration and adhesive on wet bonding performance is similar to those of the dry bonding performance, that is, the specimens of configuration D has the highest shear strength and WFP. In particular, the WFP of configuration D was close to 100% after treatment. In addition, after treatment, the bonding performance of all specimens decreased. Compared with the dry bonding performance, the reduction rate of BSS and WFP of the PRF specimens was the lowest (19.02% and 5.37%), followed by the EPI specimens (22.33% and 9.80%), and the highest was the PUR specimens (26.79% and 13.33%).

The results of two-way ANOVA for BSS and WFP properties are summarized in Table 5. It can conclude that the configuration had significant effect on all the BSS and WFP. However, the adhesive only had a significant effect on the WFP at dry conditions and it only had a significant effect on BSS at wet conditions. Furthermore, the configuration and adhesive had significant cross influence.

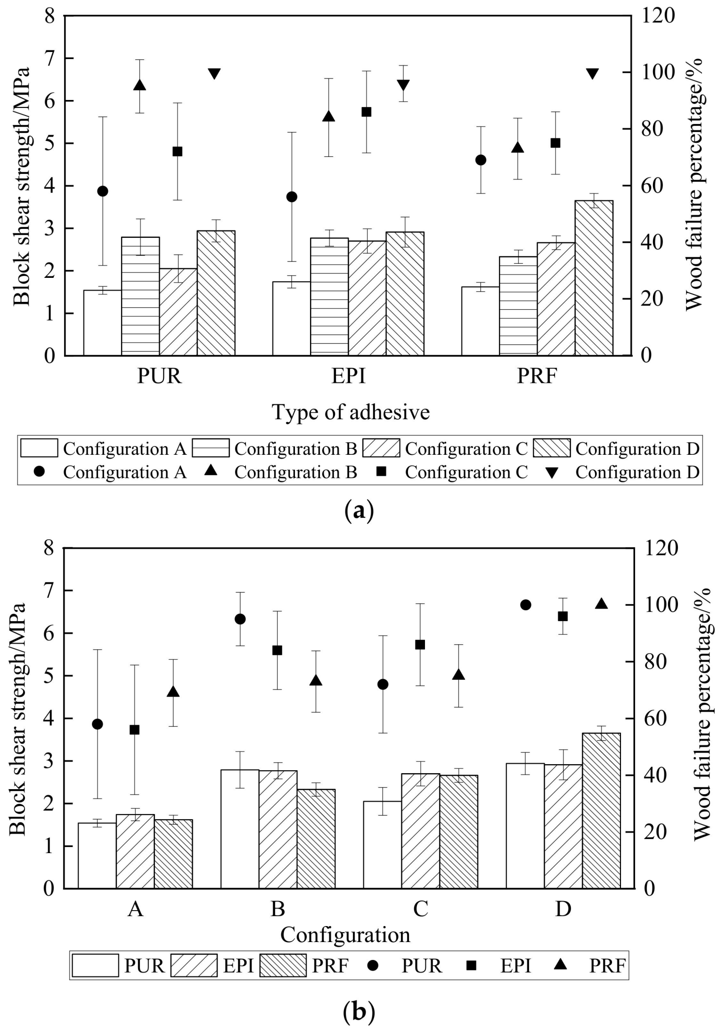

Figure 5. BSS and WFP of CLT and HCLT specimens at wet condition: (**a**) Influence of configuration, and (**b**) Influence of adhesive.

Table 5. ANOVA results of BSS and WFP.

	Source of Variance	df	Mean Square	Significant Level
BSS at dry condition	configuration	3	24.898	***
	adhesive	2	0.162	ns
	configuration × adhesive	6	0.279	ns
WPF at dry condition	configuration	3	2616.416	***
	adhesive	2	932.176	***
	configuration × adhesive	6	143.441	ns
BSS at wet condition	configuration	3	10.770	***
	adhesive	2	0.538	***
	configuration × adhesive	6	0.931	***
WPF at wet condition	configuration	3	7078.994	***
	adhesive	2	17.502	ns
	configuration × adhesive	6	720.533	**

ns = not significant, * = significant at 5% level, ** = significant at 1% level, *** = significant at 0.1% level.

Three typical failure modes of specimens occurred during the block shear tests, Figure 6. Most of the SPF CLT specimens occurred shear failure of SPF dimension lumber near the bonding line, Figure 6a. Regarding the COSB HCLT specimen, except the shear failure of COSB near the bonding line, Figure 6b,d, the shear failures were prone to occur in the middle of COSB lamination thickness, Figure 6c,e. This is because there is density profile along the thickness direction of COSB and the density is lowest in the middle of COSB lamination thickness, which resulting into shear failure.

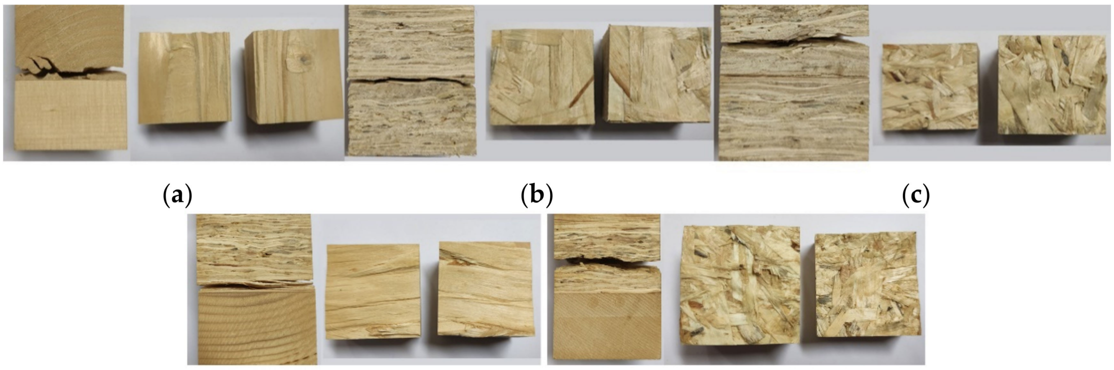

Figure 6. Typical failure modes of CLT and HCLT specimens during block shear tests.

3.2.2. Rate of Delamination

The RD results of all specimens are shown in Table 2. The average impregnation RD-1 cycle and RD-2 cycle of all specimen were 3.17% and 7.56%, respectively, and the boiling RD-1 cycle and RD-2 cycle of all specimen were 6.24% and 12.05%, respectively. In addition, the boiling RD of the specimens was higher than that of the impregnation RD, such as the average RD-1 cycle and RD-2 cycle of the boiling specimens were 96.64% and 59.45% higher than those of impregnation specimens. This is mainly due to the more times of impregnation and the higher temperature of the impregnation, water is easier to enter the adhesive interface, thus leading to a greater RD value [27].

The ANOVA results of RD values shown that only adhesive had a significant effect on the impregnation and boiling RD-2 cycle value, Table 6. The configuration had no significant effect on the RD value. Under the four treatment conditions, the PRF specimens had the minimum RD value meanwhile the EPI specimens had the maximum RD value.

Table 6. ANOVA results of RD.

	Source of Variance	df	Mean Square	Significant Level
Impregnation-1 cycle	configuration	3	8.997	ns
	adhesive	2	20.869	ns
	configuration × adhesive	6	3.074	ns
Impregnation-2 cycle	configuration	3	15.567	ns
	adhesive	2	55.118	***
	configuration × adhesive	6	13.438	ns
Boiling-1 cycle	configuration	3	15.567	ns
	adhesive	2	55.118	ns
	configuration × adhesive	6	13.438	ns
Boiling-2 cycle	configuration	3	23.152	ns
	adhesive	2	338.330	*
	configuration × adhesive	6	16.291	ns

ns = not significant, * = significant at 5% level, *** = significant at 0.1% level.

During the impregnation and boiling process, in addition to the delamination of the bonding lines, two other failure modes also occurred, Figure 7. Since the density and internal bonding strength in the middle of COSB lamination thickness are the lowest, cracks are prone to occur there, Figure 7. Moreover, the width of gaps between SPF dimension lumber in the same layer became large, and even cracks were prone to happened there during the impregnation and boiling process, Figure 7. At present, most of CLT products employ no edge-gluing and exist gaps between laminations at the same layer, which help to reduce the warp and cost of CLT products [28]. Several studies have studied the effects of gaps on the physical and mechanical properties of CLT, such as the rolling shear and bending properties, and connection performance. However, most of these researches evaluated the CLT specimens without treatments [29–32]. In this study, we found during the cyclic treatment of impregnation and drying, water was prone to enter from the gaps. By the combined action of shrinkage and swelling of the lamination, the width of gaps increased. Based on the experimental results here, for the long-term application of CLT products, attention should be paid to the change of gap width between laminates and its influence on the physical and mechanical properties, and the appearance of CLT.

Figure 7. Typical failure modes of CLT and HCLT specimens during delamination tests.

4. Conclusions

The main findings are summarized as follows:

(1) Dimensional stability. The addition of COSB reduced the WA of the HCLT specimen, but increased the TS value. The configuration and adhesive had a significant impact on the dimensional stability of the specimen. The effect of COSB on the dimensional stability of HCLT specimen should be comprehensively considered.

(2) Bonding performance. The BSS and WFP of HCLT specimens at dry and wet conditions were higher than those of SPF CLT specimens, especially for the configuration D. The configuration significantly affected the BSS and WFP of specimen. The values of RD-2 cycle were higher than the values of RD-1 cycle, and the PRF specimen had the lowest RD value in the three adhesives specimens.

(3) Failure modes. Due to the density profile of COSB panel, failure was prone to occur in the middle of COSB lamination thickness during the block shear and delamination tests. In addition, the width of the gaps between the SPF dimension lumber at the same lamination became large after delamination tests.

Author Contributions: Z.L.: Methodology, Investigation, Writing—original draft, Formal analysis, Visualization. G.C.: Methodology, Investigation, Formal analysis, Visualization. Y.W.: Validation, Visualization. Z.W.: Conceptualization, Resources, Writing—review & editing, Supervision, Project administration, Funding acquisition. M.G.: Conceptualization, Writing—review & editing. All authors have read and agreed to the published version of the manuscript.

Funding: This work has been carried out as parts of projects entitled 'National Key Research and Development Program of China' (2021YFD2200605), 'National Natural Science Foundation of China' (32071700 and 31570559) and Qing Lan Project.

Institutional Review Board Statement: Not applicable.

Informed Consent Statement: Not applicable.

Data Availability Statement: No further data is available.

Acknowledgments: The authors wish to acknowledge the National Key Research and Development Program of China (2021YFD2200605), the National Natural Science Foundation of China (32071700 and 31570559), and Qing Lan Project. The authors would also like to thank TIANXIN TIMBER FRANED BUILDING for testing materials and technical advices.

Conflicts of Interest: The authors declare no conflict of interest.

References

1. Muszynski, L.; Hansen, E.; Fernando, S.; Schwarzmann, G.; Rainer, J. Insights into the global cross-laminated timber industry. *BioProducts Bus.* **2017**, *2*, 77–92.
2. Pang, S.-J.; Ahn, K.-S.; Kang, S.G.; Oh, J.-K. Prediction of withdrawal resistance for a screw in hybrid cross-laminated timber. *J. Wood Sci.* **2020**, *66*, 79–90. [CrossRef]
3. Davids, W.G.; Willey, N.; Lopez-Anido, R.; Shaler, S.; Gardner, D.; Edgar, R.; Tajvidi, M. Structural performance of hybrid SPFs-LSL cross-laminated timber panels. *Constr. Build. Mater.* **2017**, *149*, 156–163. [CrossRef]
4. Wang, Z.; Fu, H.; Gong, M.; Luo, J.; Dong, W.; Wang, T.; Chui, Y.H. Planar shear and bending properties of hybrid CLT fabricated with lumber and LVL. *Constr. Build. Mater.* **2017**, *151*, 172–177. [CrossRef]
5. Gong, M. Lumber-based mass timber products in construction. In *Timber Buildings and Sustainability*; IntechOpen: London, UK, 2019.
6. Yusoh, A.S.; Tahir, P.M.; Uyup, M.K.A.; Lee, S.H.; Husain, H.; Khaidzir, M.O. Effect of wood species, clamping pressure and glue spread rate on the bonding properties of cross-laminated timber (CLT) manufactured from tropical hardwoods. *Constr. Build. Mater.* **2020**, *273*, 121721. [CrossRef]
7. Sikora, K.S.; McPolin, D.O.; Harte, A.M. Effects of the thickness of cross-laminated timber (CLT) panels made from Irish Sitka spruce on mechanical performance in bending and shear. *Constr. Build. Mater.* **2016**, *116*, 141–150. [CrossRef]
8. O'Ceallaigh, C.; Sikora, K.S.; Harte, A.M. The influence of panel lay-up on the characteristic bending and rolling shear strength of CLT. *Buildings* **2018**, *8*, 114. [CrossRef]
9. Sikora, K.S.; McPolin, D.; Harte, A.M. Shear strength and durability testing of adhesive bonds in cross-laminated timber. *Adhesion* **2016**, *92*, 758–777. [CrossRef]
10. Liao, Y.; Tu, D.; Zhou, J.; Zhou, H.; Yun, H.; Gu, J.; Hu, C. Feasibility of manufacturing cross-laminated timber using fast-grown small diameter eucalyptus lumbers. *Constr. Build. Mater.* **2017**, *132*, 508–515. [CrossRef]
11. Yusof, N.M.; Tahir, P.M.; Roseley, A.S.M.; Hua, L.S.; Halip, J.A.; James, R.M.S.; Ashaari, Z. Bond integrity of cross laminated timber from *Acacia mangium* wood as affected by adhesive types, pressing pressures and loading direction. *Int. J. Adhes. Adhes.* **2019**, *94*, 24–28. [CrossRef]
12. Wetzig, M. *Studies on the Optimization of Bonding Hardwoods*; Swiss Federal Institute of Technology in Zurich: Zurich, Switzerland; University of Cooperative Education Sachsen: Dresden, Germany, 2009.
13. Santos, P.; Correia, J.R.; Godinho, L.; Dias, A.M.P.G.; Dias, A. Bonding quality assessment of cross-layered Maritime pine elements glued with one-component polyurethane adhesive. *Constr. Build. Mater.* **2019**, *211*, 571–582. [CrossRef]
14. Knorz, M.; Torno, S.; Kuilen, J.V.D. Bonding quality of industrially produced cross-laminated timber (CLT) as determined in delamination tests. *Constr. Build. Mater.* **2017**, *133*, 219–225. [CrossRef]
15. Song, Y.J.; Hong, S. Evaluation of bonding strength of larch cross-laminated timber. *J. Korean Wood Sci. Technol.* **2016**, *44*, 607–615. [CrossRef]
16. Pang, S.-J.; Jeong, G.Y. Swelling and shrinkage behaviors of cross-laminated timber made of different species with various lamina thickness and combinations. *Constr. Build. Mater.* **2020**, *240*, 117924. [CrossRef]
17. Yusof, N.M.; Tahir, P.; Lee, S.H.; Khan, M.A.; James, R.M.S. Mechanical and physical properties of cross-laminated timber made from *Acacia mangium* wood as function of adhesive types. *J. Wood Sci.* **2019**, *65*, 20. [CrossRef]
18. Srivaro, S.; Pásztory, Z.; Le Duong, H.A.; Lim, H.; Jantawee, S.; Tomad, J. Physical, mechanical and thermal properties of cross laminated timber made with coconut wood. *Eur. J. Wood Wood Prod.* **2021**, *79*, 1519–1529. [CrossRef]
19. Li, Q.; Wang, Z.; Liang, Z.; Li, L.; Gong, M.; Zhou, J. Shear properties of hybrid CLT fabricated with lumber and OSB. *Constr. Build. Mater.* **2020**, *261*, 120504. [CrossRef]
20. Song, H.; Wang, Z.; Gong, Y.; Li, L.; Zhou, J.; Gong, M. Low-cycle fatigue life and duration-of-load effect for hybrid CLT fabricated from lumber and OSB. *J. Build. Eng.* **2022**, *46*, 103832. [CrossRef]
21. *ASTM D1037*; Standard Test Methods for Evaluating Properties of Wood Base Fiber and Particle Panel Materials. American Society for Testing and Materials: West Conshohocken, PA, USA, 2012.
22. *EN 16351*; Timber Structures cross Laminated Timber-Requirements. European Committee for Standardization: Brussels, Belgium, 2015. (In Chinese)
23. *GB/T 50329*; Standard for Test Methods of Timber Structures. Standardization Administration of China: Beijing, China, 2012. (In Chinese)
24. *GB/T 26899*; Structural Glued Laminated Timber. Standardization Administration of China: Beijing, China, 2011. (In Chinese)
25. Da Rosa, T.S.; Trianoski, R.; Iwakiri, S.; Bonduelle, G.M.; Guimarães, C.D.C. Optimization of properties of *eucalyptus* oriented strand boards by specific gravity of panels. *Maderay Bosques* **2018**, *24*. [CrossRef]
26. Papadopoulos, N.; Traboulay, E. Dimensional stability of OSB made from acetylated Fir strands. *HolzalsRohund Werkst.* **2002**, *60*, 84–87. [CrossRef]
27. Konnerth, J.; Harper, D.; Lee, S.-H.; Rials, T.G.; Gindl, W. Adhesive penetration of wood cell walls investigated by scanning thermal microscopy. *Holzforschung* **2008**, *62*, 91–98. [CrossRef]
28. Brandner, R.; Flatscher, G.; Ringhofer, A.; Schickhofer, G.; Thiel, A. Cross laminated timber (CLT): Overview and development. *Eur. J. Wood Wood Prod.* **2016**, *74*, 331–351. [CrossRef]

29. Wang, Z.; Zhou, J.; Dong, W.; Yao, Y.; Gong, M. Influence of technical characteristics on the rolling shear properties of cross laminated timber by modified planar shear tests. *Maderas Cienc. Tecnol.* **2018**, *20*, 469–478. [CrossRef]
30. Gui, T.; Cai, S.; Wang, Z.; Zhou, J. Influence of aspect ratio on rolling shear properties of fast-grown small diameter eucalyptus lumber. *J. Renew. Mater.* **2020**, *8*, 1053–1066. [CrossRef]
31. Li, X.; Ashraf, M.; Subhani, M.; Kremer, P.; Kafle, B.; Ghabraie, K. Experimental and numerical study on bending properties of heterogeneous lamella layups in cross laminated timber using Australian Radiata Pine. *Constr. Build. Mater.* **2020**, *247*, 118525. [CrossRef]
32. Brandner, R.; Ringhofer, A.; Grabner, M. Probabilistic models for the withdrawal behavior of single self-tapping screws in the narrow face of cross laminated timber (CLT). *Eur. J. Wood Wood Prod.* **2018**, *76*, 13–30. [CrossRef]